THE HENRYK NIEWODNICZAŃSKI
INSTITUTE OF NUCLEAR PHYSICS
POLISH ACADEMY OF SCIENCES

New Nanoparticles for Potential Theranostic Application

Kamil Stachurski

kamil.stachurski@ifj.edu.pl

PhD Seminar 26.04.2024

Department of Magnetic Resonance Imaging

Institute of Nuclear Physics Polish Academy of Sciences

Content

- Magnetic Resonance Imaging
- Contrast Agents
- Theranostics
- Materials and Methods
- Results
- Summary

- *This work was partially supported by the National Centre of Science (NCN) of Poland, under grant nr: 2019/34/H/ST5/00578 (GRIEG-1, funded under the Norwegian Financial Mechanism) and grant nr. 2020/39/B/NZ7/01913 (OPUS 20).*

Derrick Kaseman et al.

Magnetic Resonance Imaging

- Nuclei which have a non-zero spin possess a magnetic moment, which is proportional to angular momentum:

$$\mu_z = \gamma \hbar m$$

- Equilibrium distribution is a descripted by the Boltzmann distribution:

$$\frac{N^{\uparrow}}{N^{\downarrow}} = \exp[-\frac{\Delta E}{k_B T}]$$

- The difference between energy levels can be described as:

$$\Delta E = \gamma \hbar B_0$$

- Larmor frequency:

$$\omega_0 = \gamma B_0$$

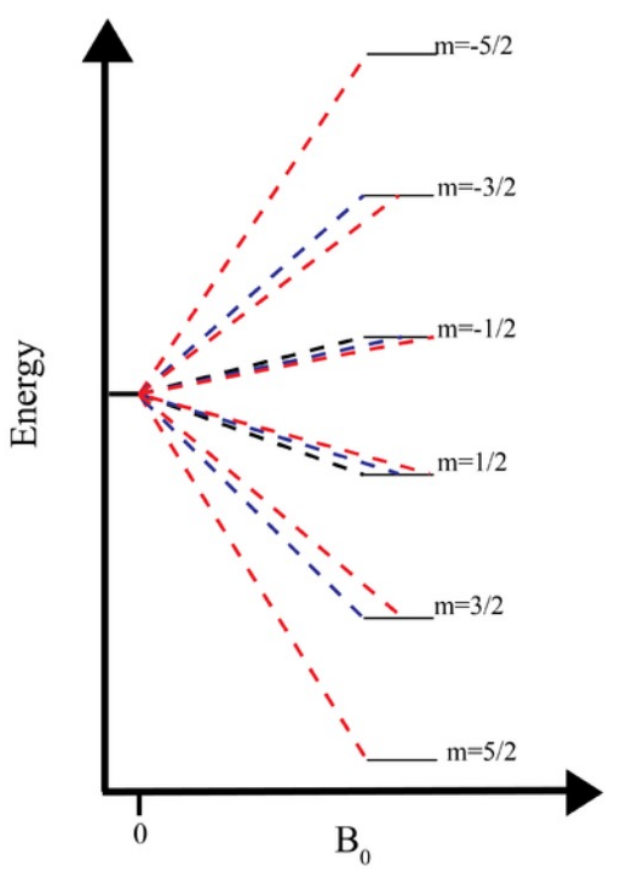

Figure 1. Allowed energy levels for atomic nuclei with different values of magnetic spin quantum number.

Natalia Łopuszyńska, 2021
Allen D. Elster, 2024

Magnetic Resonance Imaging

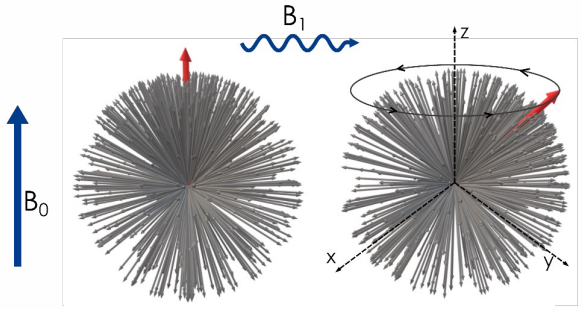

Figure 2. Distribution of spin orientation in absence and in presence B_1 magnetic field.

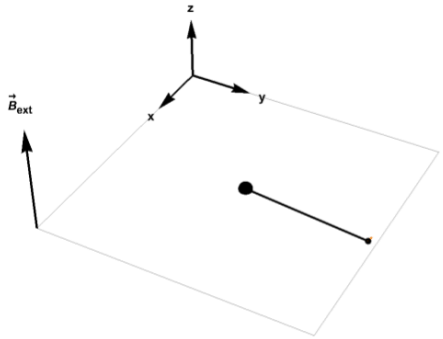

Figure 3. Evolution of magnetization vector in magnetic field.

$$M_x(t) = e^{-t/T_2}\left[M_x(0)cos\omega_0 t + M_y(0)sin\omega_0 t\right]$$

$$M_y(t) = e^{-t/T_2}\left[M_y(0)cos\omega_0 t + M_x(0)sin\omega_0 t\right]$$

$$M_z(t) = M_z(0)e^{-\frac{t}{T_1}} + M_0(1 - e^{-\frac{t}{T_1}})$$

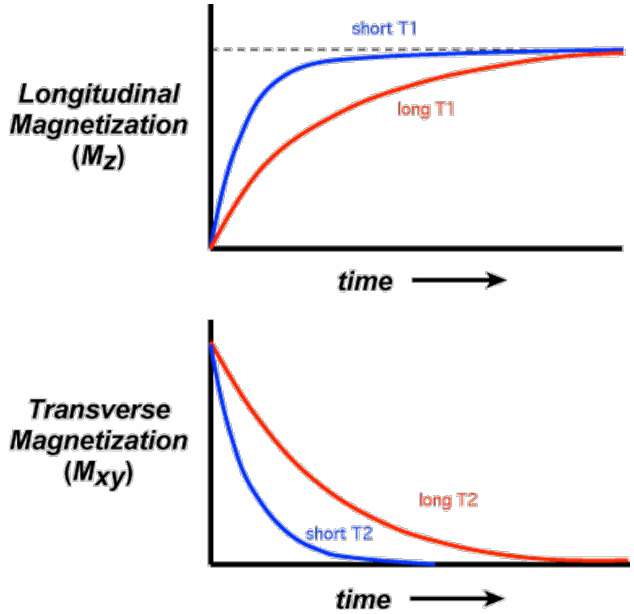

Figure 4. Longitudinal and transverse relaxation curves described by relaxation times..

Adel Razek et al., 2018

Magnetic Resonance Imaging

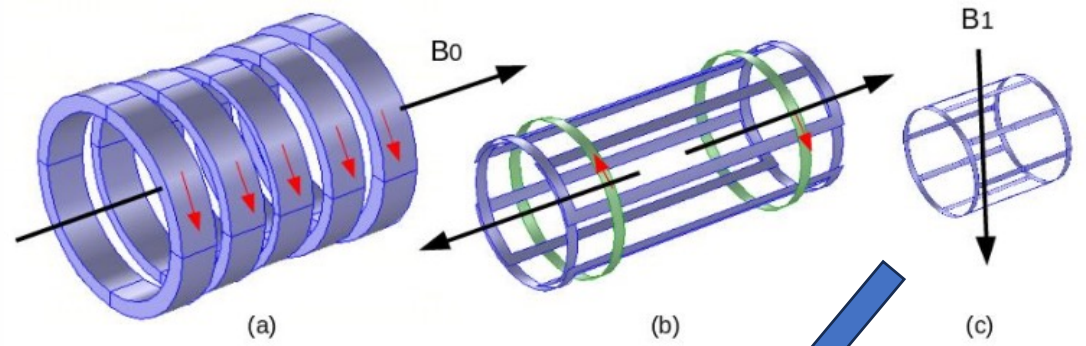

$$\omega_0 = \gamma B_0$$

γ – giromagnetic ratio
B_0 - external magnetic field

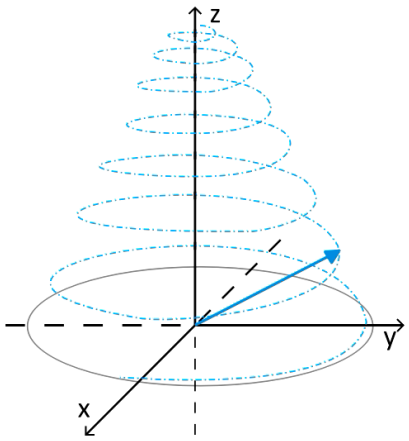

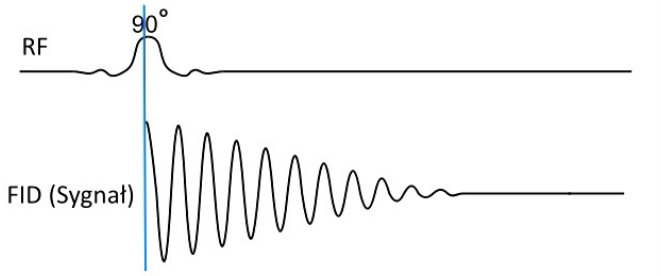

Figure 5. Principle of MRI.

Allen D. Elster, 2024

Magnetic Resonance Imaging

$$k_x = \frac{\gamma}{2\pi}\int_0^t G_z(t')dt'$$

$$k_y = \frac{\gamma}{2\pi}\int_0^t G_y(t')dt'$$

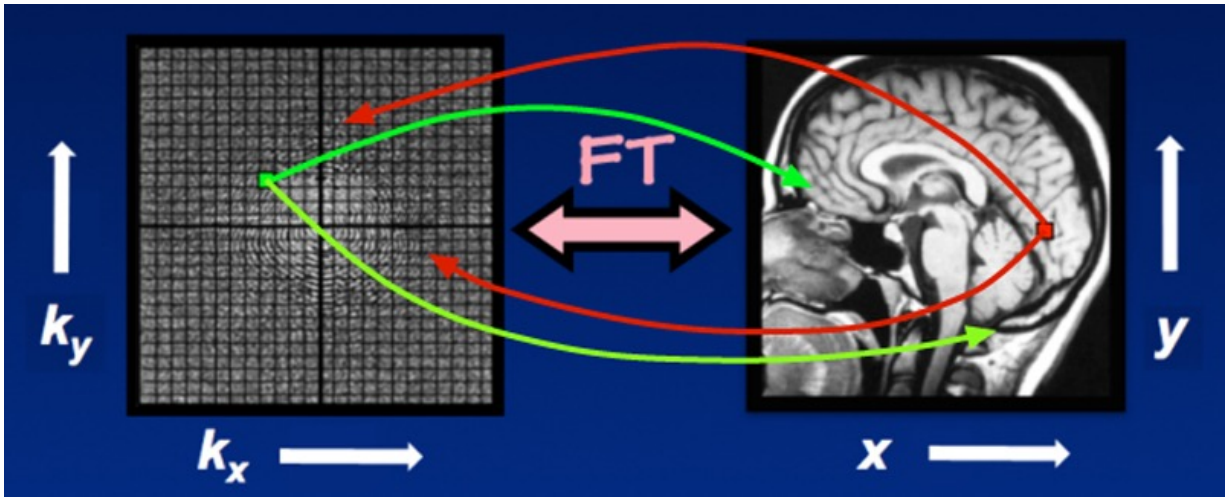

Figure 6. Representation of K-Space and Fourier transform.

Source: https://www.youtube.com/watch?v=TQegSF4ZiIQ

Magnetic Resonance Imaging

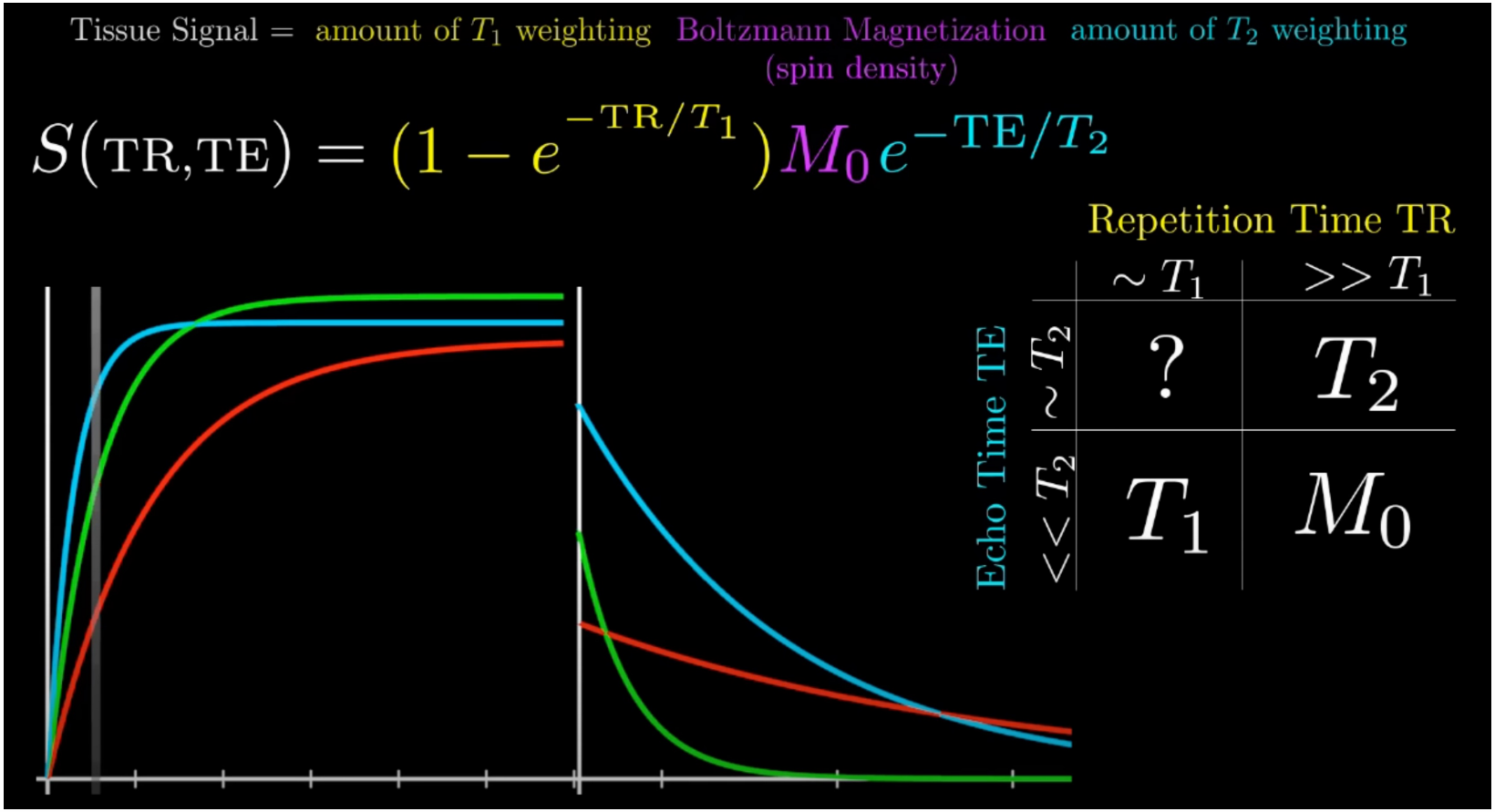

Figure 7. MRI signal equation and their contrast function depends on TR and TE..

David C. Preston, 2006

Magnetic Resonance Imaging

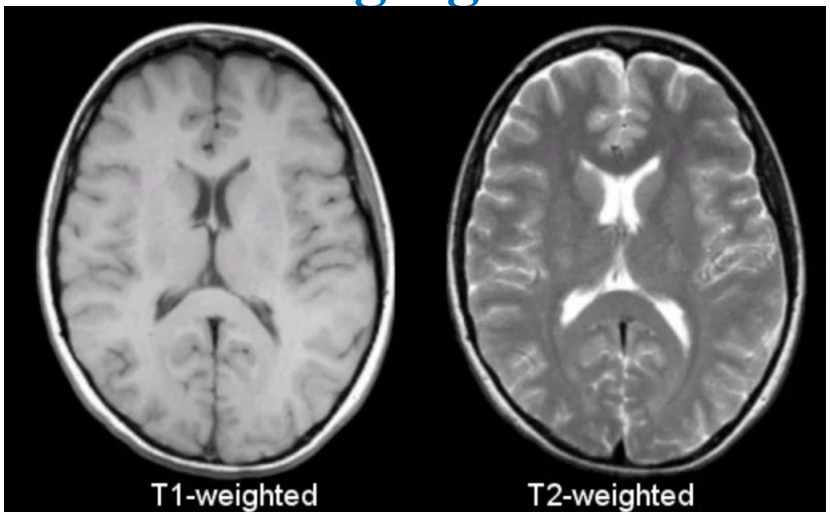

Figure 8. T_1- and T_2-weighted MR image of human brain.

Tissue	T1-Weighted	T2-Weighted
CSF	Dark	Bright
White Matter	Light	Dark Gray
Cortex	Gray	Light Gray
Fat (within bone marrow)	Bright	Light
Inflammation (infection, demyelination)	Dark	Bright

Contrast Agents

Mike Jeon et al. Advanced Materials, 2020
Ulrich Flögel et al. Circulation, 2008;118:140-148

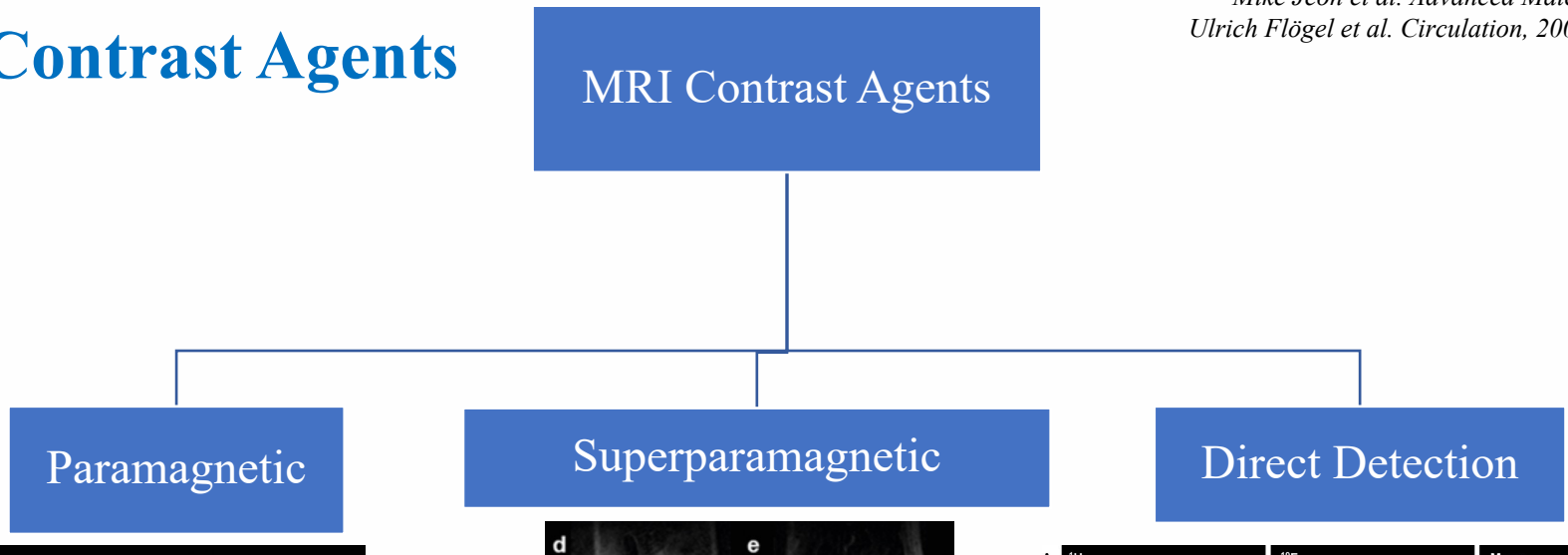

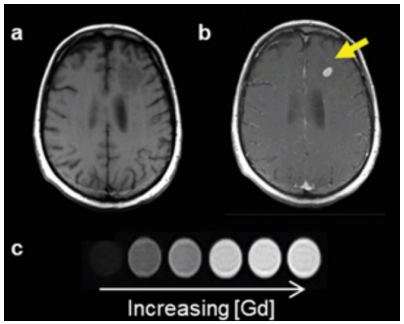

Figure 9. T_1-weighted images of human brain with gadolinium based contrast agent.

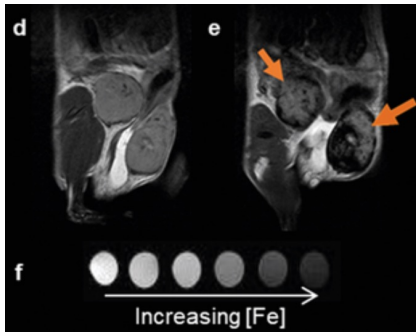

Figure 10. T_2-weighted images of inflamed mouse mammary gland tumors.

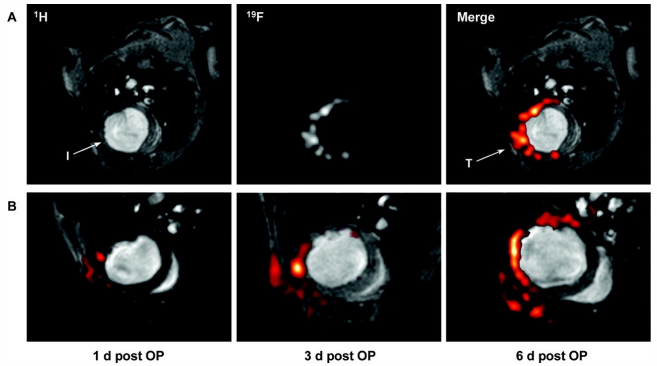

Figure 11. Infiltration of PFCs after myocardial infarction as detected by in vivo 19F MRI.

Theranostics

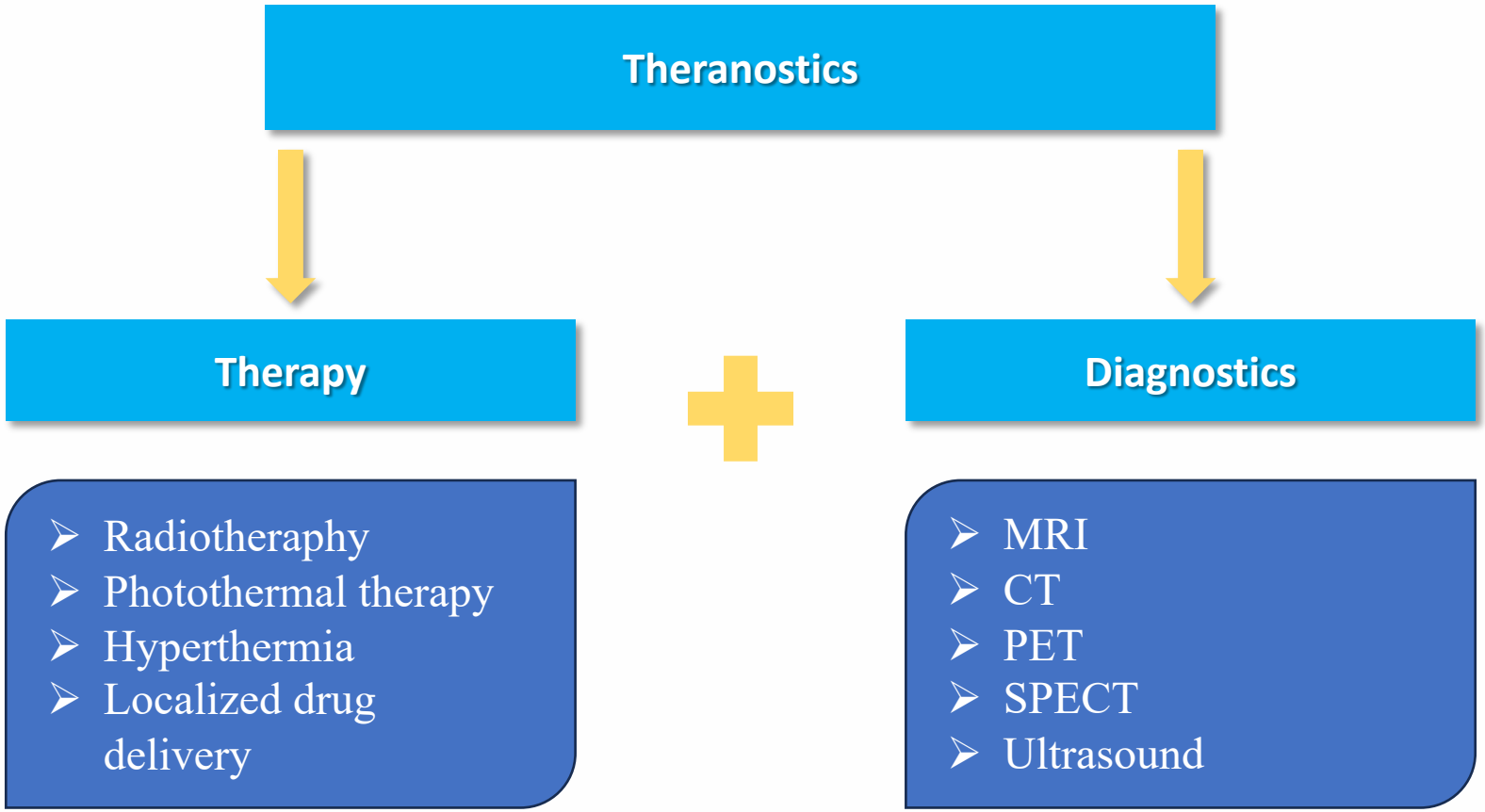

Kamil Stachurski

Materials and Methods

Polymeric NCs

- AOT/PLL with one Gd layer
- AOT/PLL with two Gd layers
- PCL with one Gd layer
- PCL with two Gd layers

HNS Nps

- HNS-Gd in PBS
- HNS-Gd in water
- Lactamide HNS-Gd
- 19F-HNS

CeO_2 NPs

- CeO_2-Gd
- CeO_2

Materials and Methods

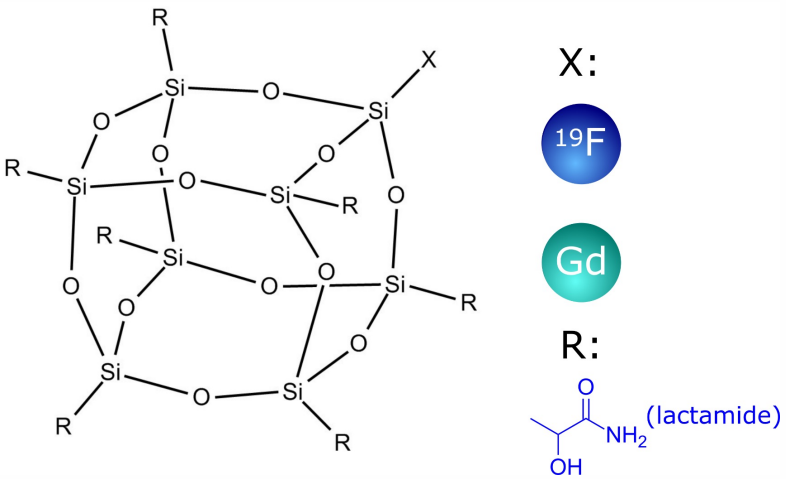

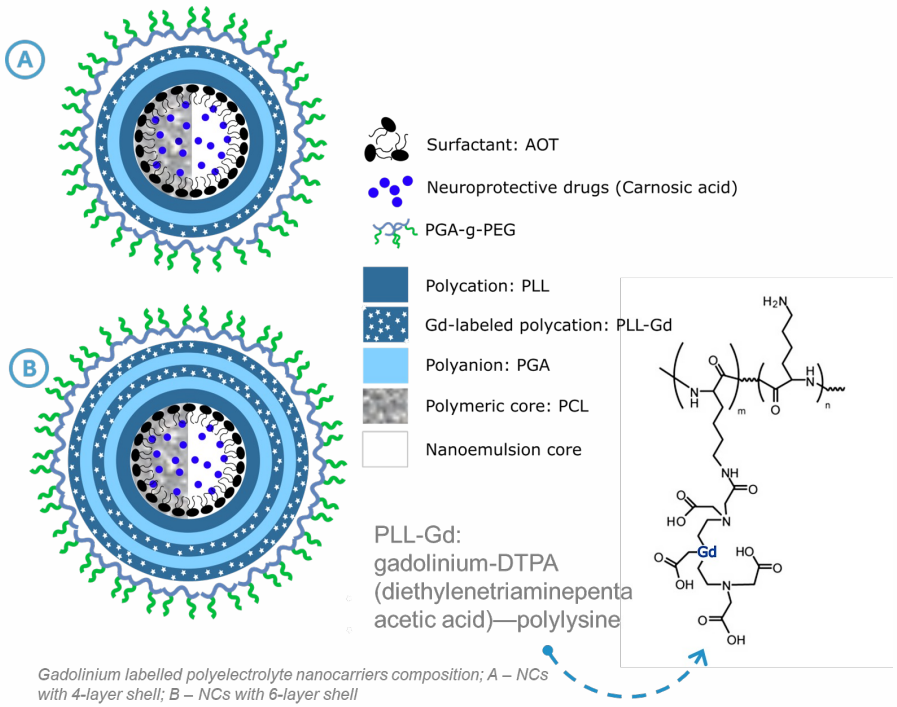

Figure 12. Schematic representation of investigated HNS and CeO_2 NPs and AOT/PCL nanocapsules.

Ilya L. Gubskiy et al. Transl. Stroke Res., 9, 417-425, 2018

Materials and Methods

- MCAO – Middle Cerebral Artery Occlusion
- Model of ischemic stroke in rats
- Insertion of a catheter into the brain
- Reduced blood flow to the brain leading to tissue damage and neurological deficits

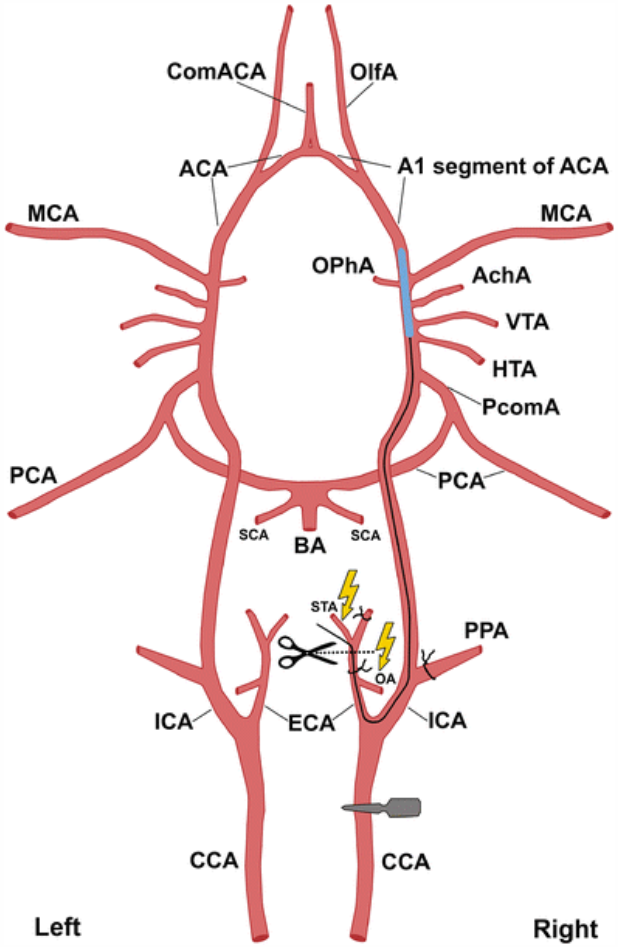

Figure 13. Schematic representation of the major rat head and neck arteries (view from the top) and the appropriate filament position during MCAO.

Materials and Methods

For RARE-VTR TR is varied to sample the T_1 relaxation curve

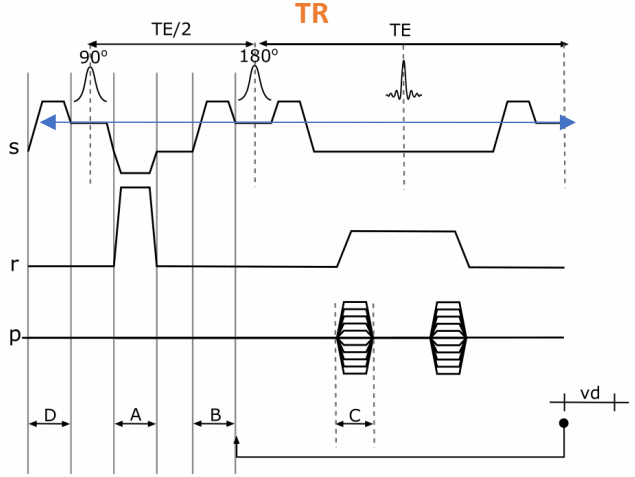

Figure 14. MSME sequence time diagram.

In Vitro Sequences Pipeline:

- T_1 map (RARE VTR)
- T_2 map (MSME)

$$\frac{1}{T_i} = \frac{1}{T_{iS}} + r_i \cdot C;\ i = (1,2)$$

T_i – measured spin-latice or spin-spin relaxation time
T_{iS} – relaxation time of the solvent nuclei without the contrast agent
C – concentration of Gd

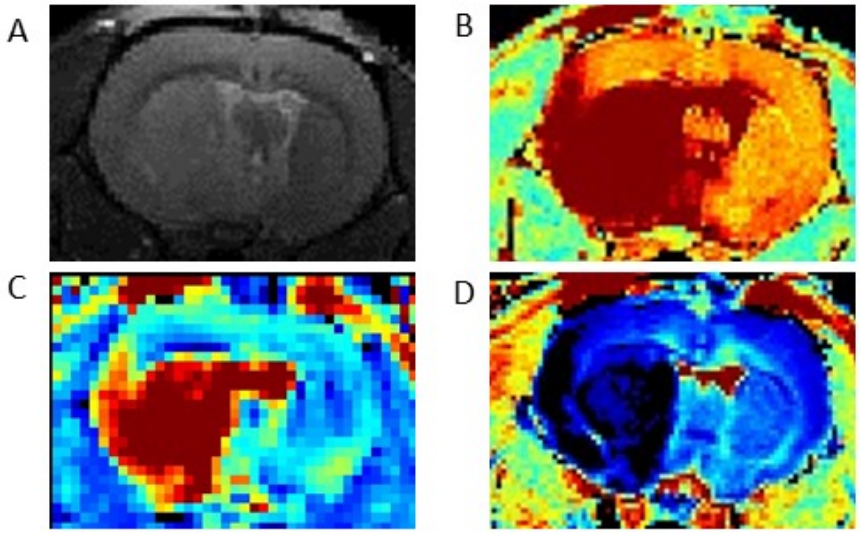

Figure 15. T2-weighted (A), T2 map (B), T1 map (C) and diffusion map (D) on rat brain with ischemic stroke model.

In Vivo Sequences Pipeline:

- T_2-weighted images
  - T_2 map
  - T_1 map
- Diffusion map
- Perfusion map
- DCE (Dynamic Contrast Enhanced)

Materials and Methods

Peter Caravan et al. Chem. Rev. 1999, 99, 2293-2352
Bloembergen N. et al. J. Chem. Phys. 1961, 34, 842-850

- The relaxation of water molecules surrounding the paramagnetic complex is induced by a fluctuating magnetic field generated by the Brownian motion of this complex and is described by the Solomon–Bloembergen–Morgan (SBM) Theory
- The presence of a gadolinium(III) complex will increase the longitudinal and transverse relaxation rates, $1/T_1$ and $1/T_2$ of solvent nuclei
- Diamagnetic and paramagnetic relaxation rates are additive and described as

$$\left(\frac{1}{T_i}\right)_{obs} = \left(\frac{1}{T_i}\right)_{d} + \left(\frac{1}{T_i}\right)_{p}$$

- The paramagnetic contribution is dependent on the concentration of paramagnetic species
- Relaxivity is defined as the slope of the concentration dependence

$$\left(\frac{1}{T_i}\right)_{obs} = \left(\frac{1}{T_i}\right)_{d} + r_i * c_{Gd}$$

Results (in vitro)

C [mM]	r1 [$mM^{-1}s^{-1}$]	
	One Gd layer	Two Gd layers
AOT/PLL	3.711	2.55
PCL	3.64	3.29

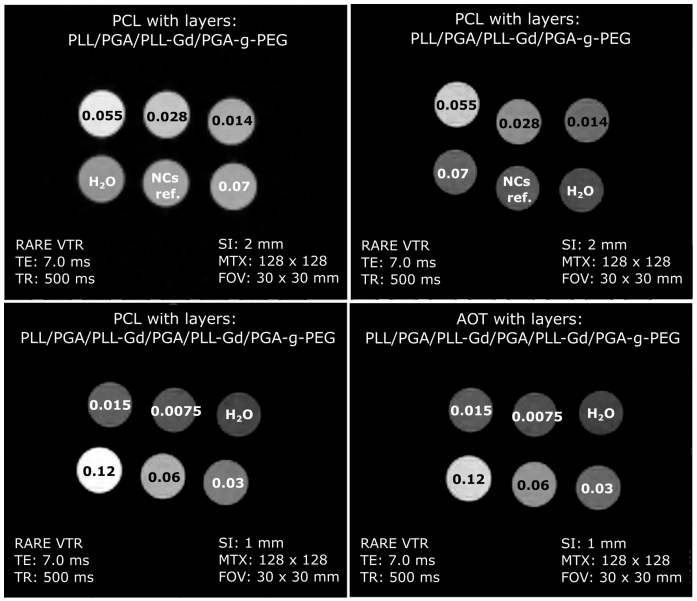

Figure 16. T_1-weighted images of AOT and PCL with one and two gadolinium layers.

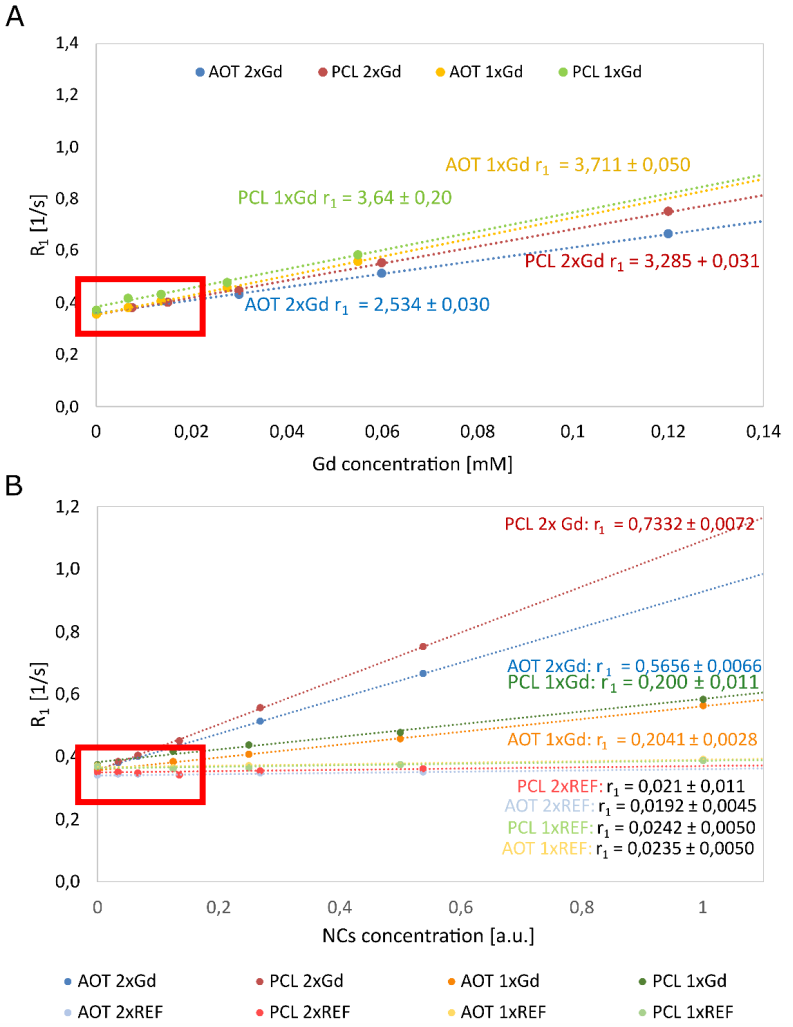

Figure 17. Molar relaxivities for AOT and PCL nanocapsules with one and two gadolinium layers.

Results (in vitro)

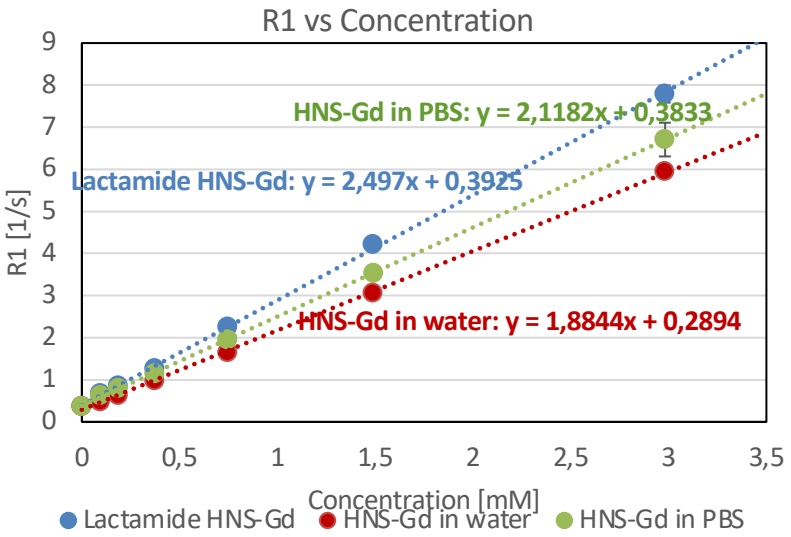

Figure 18. Molar relaxivities of HNS nanoparticles.

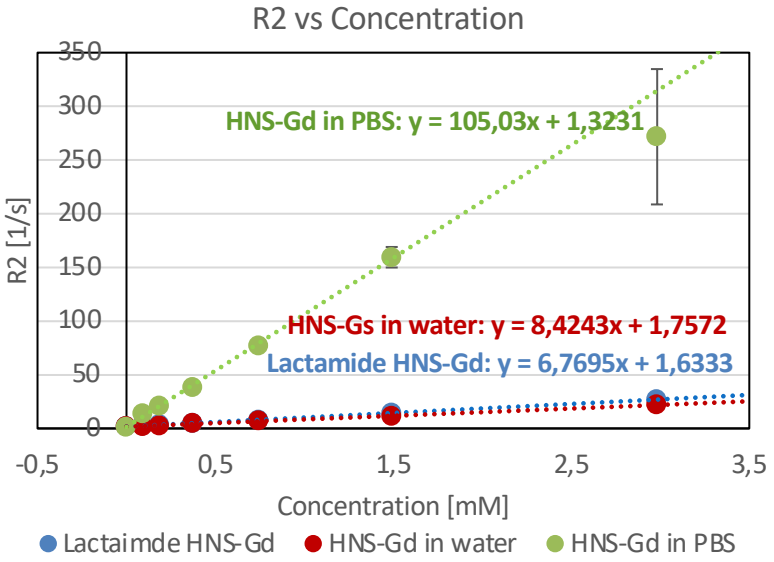

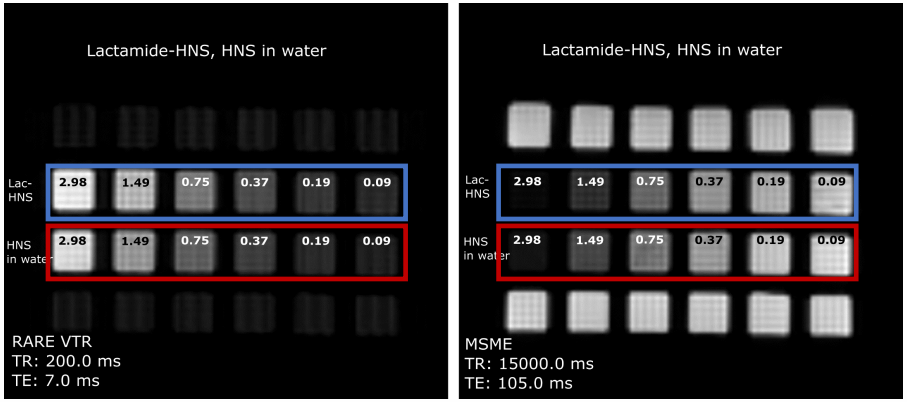

Figure 19. T_1- and T_2-weighted images of Lactamide HNS and solution in water.

Results (in vitro)

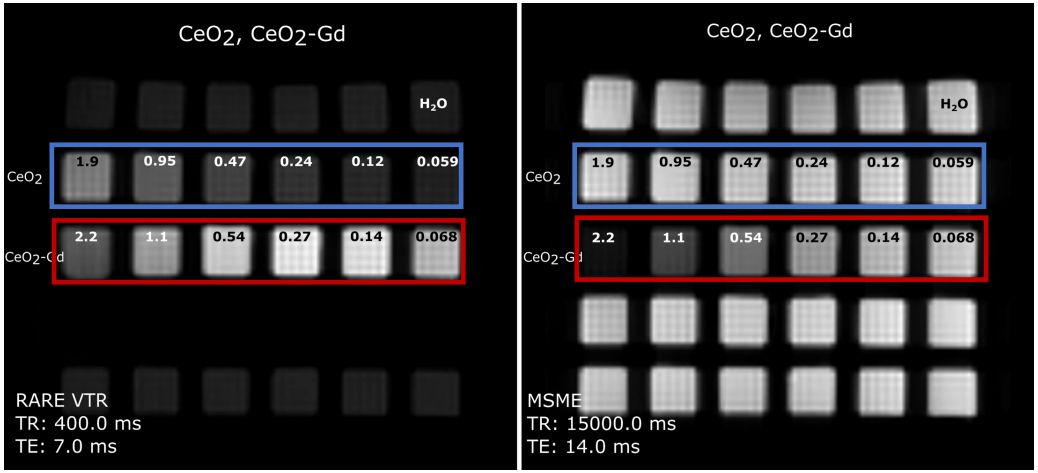

Figure 20. T_1-weighted (left row) and T_2-weighted (right row) images of samples with CeO2 NPS. Sequences and parameters as marked in the figure.

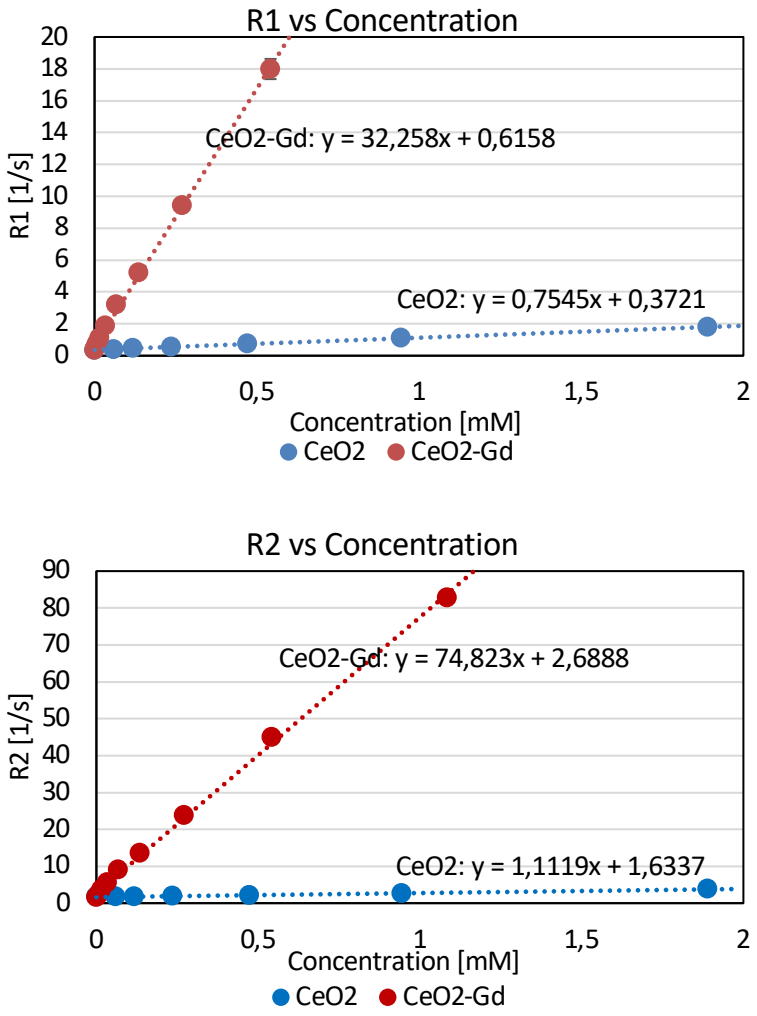

Figure 21. Molar relaxivities of CeO2 nanoparticles.

Results (in vitro)

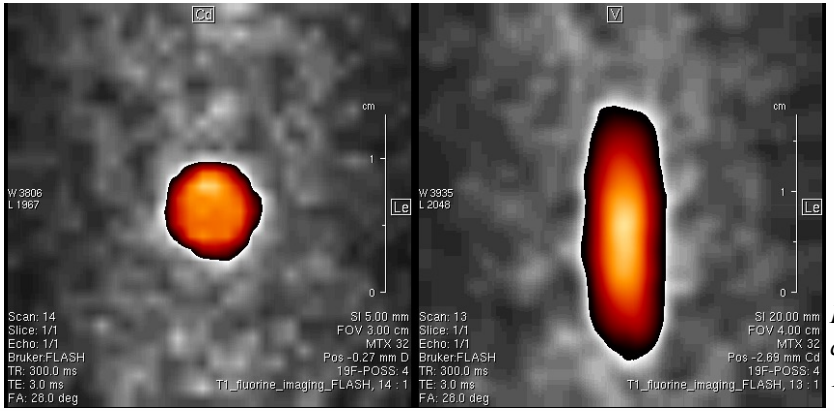

Figure 22. 19F images (two crossections) of the sample with 19F-HNS NPS

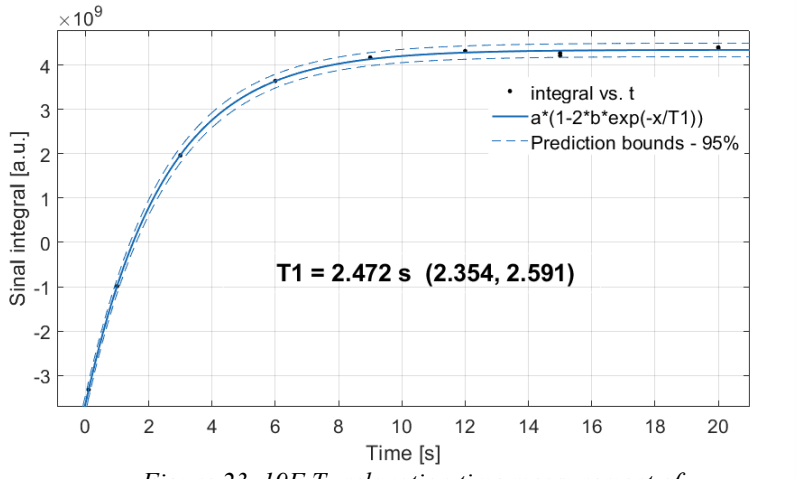

Figure 23. 19F T_1 relaxation time measurement of the sample with 19F-HNS NPS

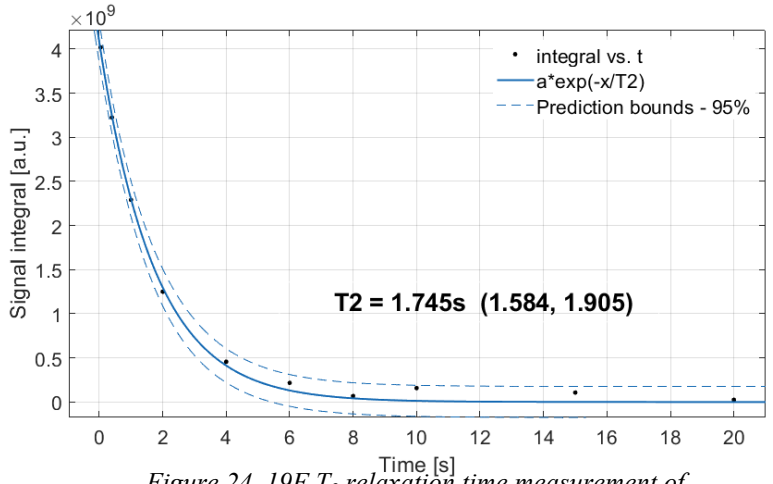

Figure 24. 19F T_2 relaxation time measurement of the sample with 19F-HNS NPS

Results (in vivo)

T1 map whole brain	T1 map in the left hemisphere	T1 map in the right hemisphere	T1 distribution in the left hemisphere	T1 distribution in the right hemisphere
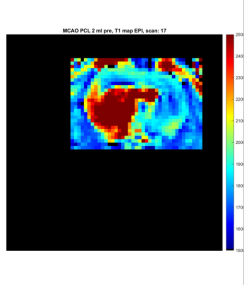	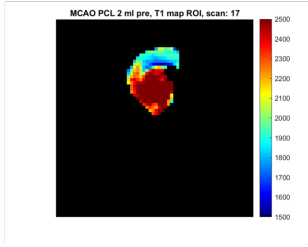	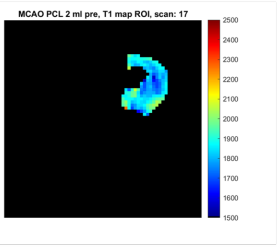	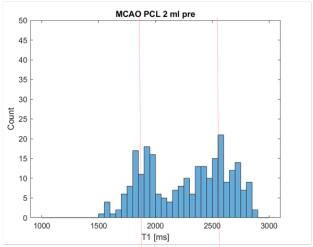	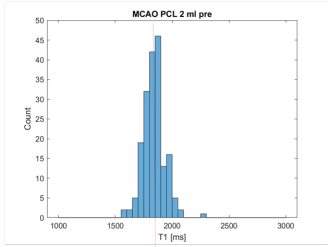
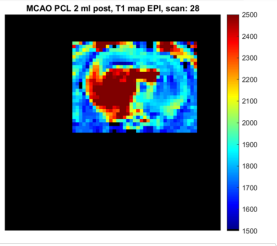	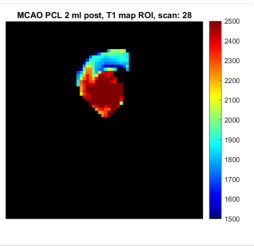	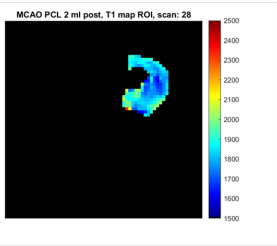	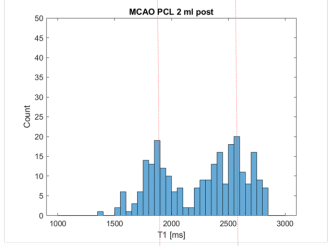	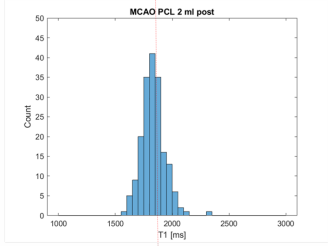
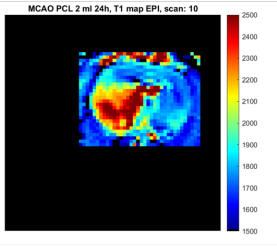	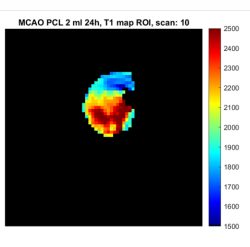	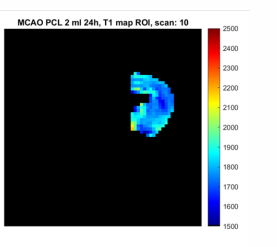	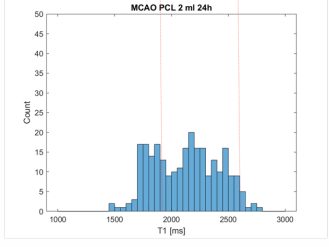	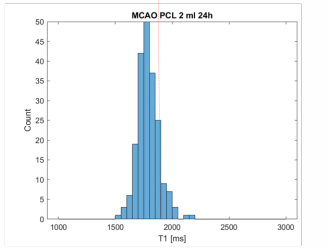

Results (in vivo)

Magnevist™

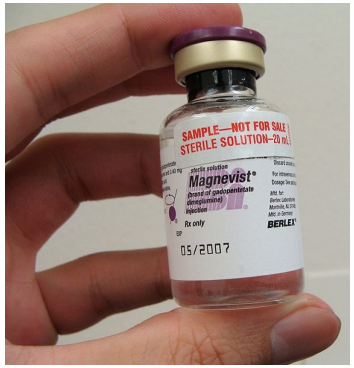

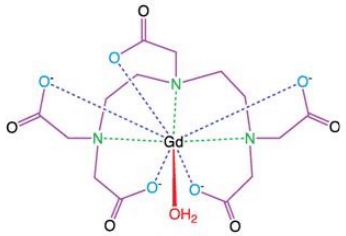

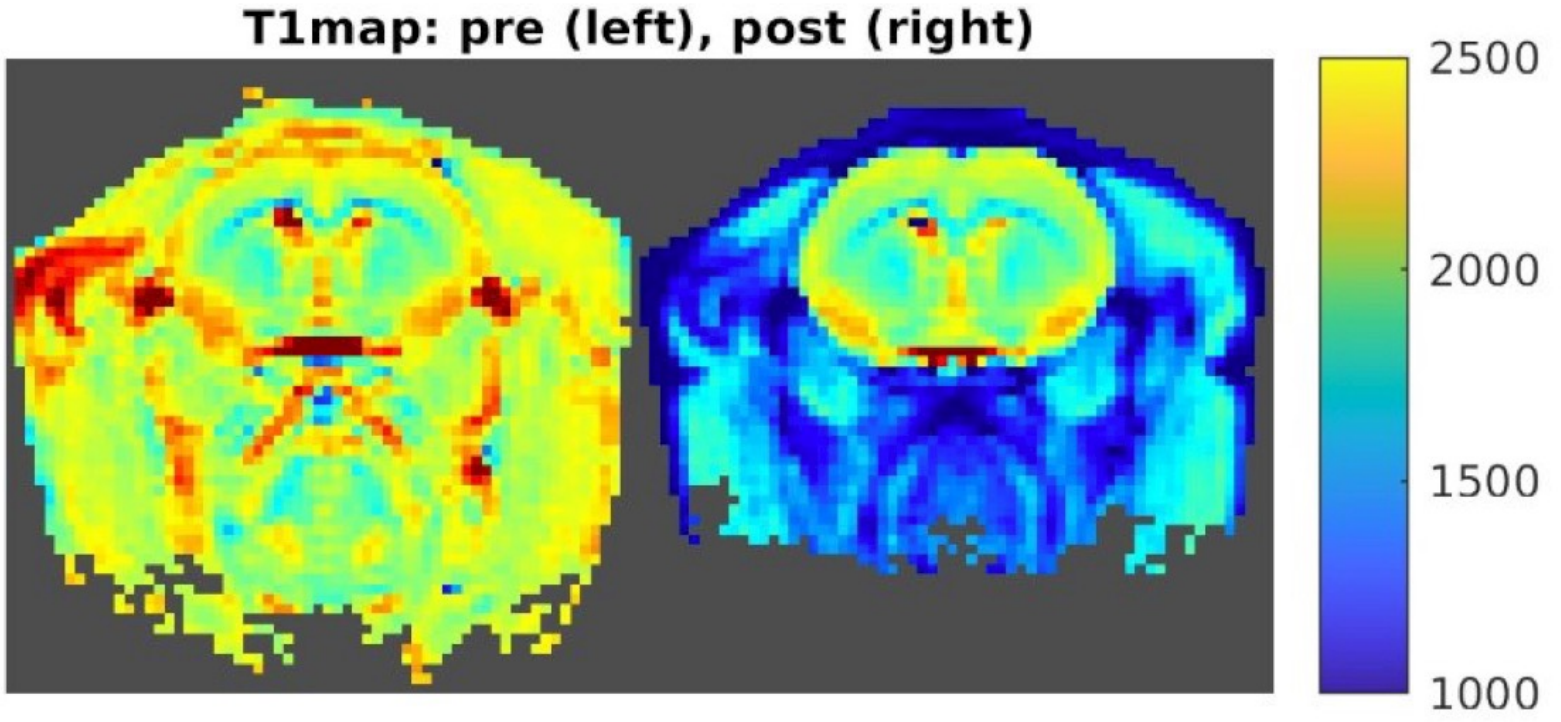

Results (in vivo)

Magnevist™
c_{Gd} = 0.5 mM

PCL NPs
c_{Gd} = 0.055 mM

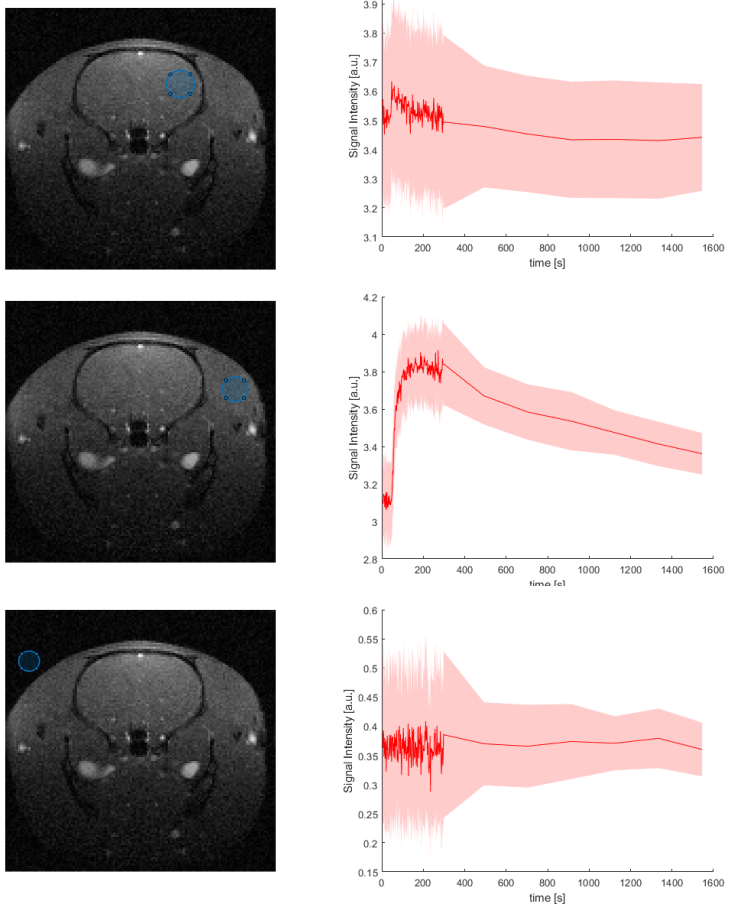

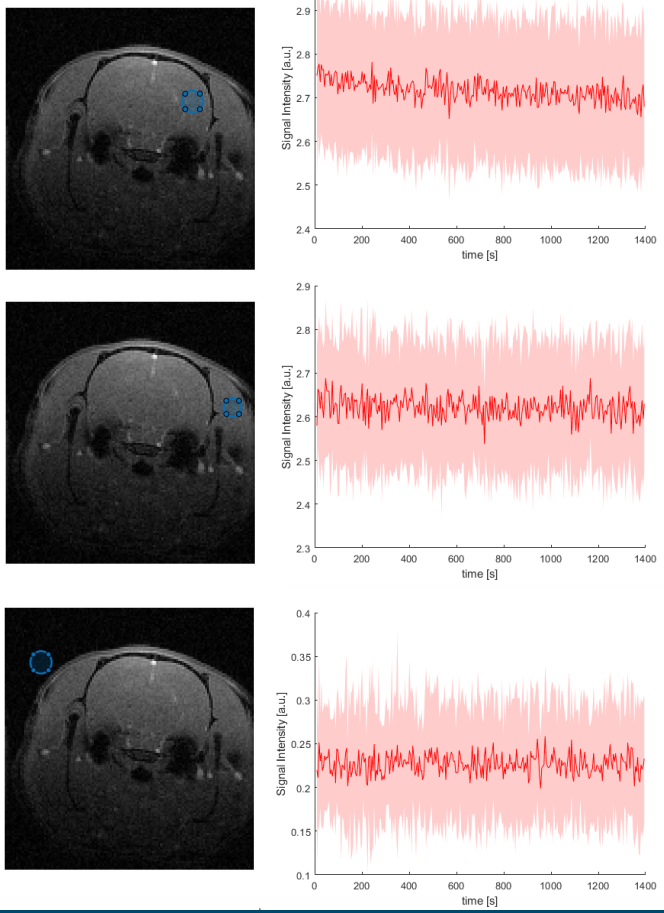

Summary

- Analysis of PCL, AOT, HNS, CeO_2 contrast properties was performed, by calculating molar relaxivities
- All HNS-based nanoparticles exhibit reasonable positive contrasting properties, with r_1 values close to 2.0 $mM^{-1}s^{-1}$.
- HNS-Gd in PBS exhibits a relatively high r_2 value of 105.03 $mM^{-1}s^{-1}$, which can be attributed to binging to PBS particles and the creation of large molecules. Such a solution has also strong cytotoxic properties, while a similar effect was not observed for HNS-Gd in water.
- CeO_2-Gd nanoparticles have excellent positive contrasting properties, described by the very high r1 value of 32 $mM^{-1}s^{-1}$ which is also greatly visible in MR images above.
- 19F-HNS exhibits preferable characteristics for 19F MRI.
- There is a difference in the distribution of the hemispheres for stroke brains.
- PCL does not accumulate in the brain because the molecules do not cross the BBB.

NPs	AOT x1 Gd	PCL x1 Gd	AOT x2 Gd	PCL x2 Gd	HNS-Gd in water	HNS-Gd in PBS	Lact. HNS-Gd	CeO2	CeO2-Gd
r_1 [$mM^{-1}s^{-1}$]	3.71	3.64	2.53	3.29	1.88	2.12	2.49	0.75	32.26
r_2 [$mM^{-1}s^{-1}$]	11.9	22.8	15.49	16.82	6.76	105.1	8.42	1.11	74.82

What’s next?

- Check relaxation properties of another nanoparticle or nanocapsules
- Conduct more in vivo experiments and precisely characterize the MCAO model
- Good BBB transport means good biodistribution
- Check neuroprotective effects
- ...

No.	Target Ligands	Targets	Properties	Carriers	References
1	PHSRN peptides	Integrin $\alpha_5\beta_1$ enriched in the cerebral vasculature of ischemic tissue	Promoting angiogenesis and reducing BBB leakage	HES	[108]
2	Cyclo (Arg-Gly-Asp-D-Tyr-Lys) peptide	Integrin $\alpha_v\beta_3$ in damaged cerebral vascular endothelial cells	-	Mesenchymal stromal cell-derived exosomes	[87,88]
3	TfR targeted peptides	TfR in cerebral cortex microvessels	A good affinity with the target and smaller in size, without immunogenicity	PGA	[95]
4	PLT membrane and Arg-Gly-Asp peptides	Damaged and angiogenic blood vessels	-	PLGA	[60]
5	Neutrophil membranes	Damaged endothelial cells	Biocompatibility, long circulation times, and without immunogenicity	PLGA	[37,61]
6	Arg-Gly-Asp peptides	Integrin $\alpha_v\beta_3$ in damaged cerebral vascular endothelial cells	-	Neural progenitor cell-derived extracellular vesicles	[91,113]
7	Neutrophil membrane	Inflamed brain microvascular endothelial cells	Biocompatibility, long circulation times, and without immunogenicity	Nanozymes	[75]
8	PLT membrane	Injured vasculature endothelial cells	Biocompatibility, long circulation times, and without immunogenicity	Biomimetic nanobubble	[83]
9	Macrophage membrane	Injured vasculature endothelial cells	Long circulation times, without immunogenicity	MnO_2 nanosphere	[32]
10	Monocyte membrane	Inflammatory endothelial cells	Inhibiting the recruitment of inflammatory cells to the brain	PLGA	[34]
11	Angiopep-2	Low density lipoprotein receptor-related protein 1 receptor on the BBB	-	Micelles	[40]
12	Mannose	Microglia and macrophages	-	Curdlan nanoparticles	[99,100]
13	2- MPPA	Microglia	-	Dendrimer	[69]
14	The tripeptide agonist N-acetyl Pro-Gly-Pro	CXCR2 receptor on the membrane of neutrophil	Low immunogenicity	DGL nanoparticles	[112]
15	CFLFLF	FPR located on the surfaces of neutrophils	-	PLGA and PEG nanoparticles	[79]
16	Glutathione	The ischemic brain area	-	Nanogel	[48]
17	RVG	Ischemic brain areas	-	EVs	[46]
18	Engineering CXCR4-enriched mesenchymal stem cell membrane vesicles	CXCL 12 in damaged brain	Cutting off the infiltration of neutrophils and macrophage cells in peripheral blood	Polydopamine nanospheres	[90]
19	Sodium cholate	The brain	Enhancing the water solubility of drugs	Liposomes	[51]

PHSRN, Pro-His-Ser-Arg-Asn; BBB, blood–brain barrier; HES, hydroxyethyl starch; Arg-Gly-Asp, arginine-glycine-aspartic; TfR, transferrin receptor; PGA, c-polyglutamic acid; PLT, platelet; PLGA, poly (lactic-co-glycolic acid); MnO_2, manganese dioxide; 2-MPPA, 2-(3-mercaptopropyl) pentanedioic acid; CXCR, C-X-C motif chemokine receptor; DGL, dendrigraft poly-L-lysine; FPR, formyl peptide receptor; CFLFLF, cinnam-yl-F-(D)L-F; PEG, polyethylene glycol; RVG, rabies virus glycoprotein; EVs, extracellular vehicles; CXCL12, chemokine (C-X-C motif) ligand 12.

The research presented in this lecture was performed after obtaining the consent of the bioethics committee.

Thank you for your attention!

CONTRIBUTORS

MRI INVESTIGATIONS
Natalia Łopuszyńska[1], Kamil Stachurski[1], Krzysztof Jasiński[1], Władysław P. Węglarz[1], Lili Zhang[6], William Edward Louch[6]

MATERIALS SYNTHESIS:
Krzysztof Szczepanowicz[2], Marta Szczęch[2], Piotr Warszyński[2],
Terje Didriksen[3], Juan Yang[3], Anna Lind[3], Sacha Muller[3]

BIOSAFETY ANALYSIS:
Danuta Jantas[4], Agnieszka Basta - Kaim[4], Magdalena Regulska[4], Monika Leśkiewicz[4], Magdalena Procner[4], Władysław Lasoń[4]

ANIMAL PREPARATION:
Bartosz Pomiarny[5], Katarzyna Kalita[1]

[1] Institute of Nuclear Physics Polish Academy of Sciences, Department of Magnetic Resonance Imaging, Cracow, Poland
[2] SINTEF Industry, Department of Process Technology, Oslo, Norway
[3] Institute of Catalysis and Surface Chemistry Polish Academy of Sciences, Cracow, Poland
[4] Maj Institute of Pharmacology Polish Academy of Sciences, Cracow, Poland
[5] Jagiellonian University Medical College, Cracow, Poland
[6] Oslo University Hospital, Oslo, Norway